RADIATION EFFICIENCY AND SOUND RADIATION FIELDS OF CLASSICAL GUITARS

I A Perry School of Physics and Astronomy, Cardiff University, Cardiff, UK
B E Richardson School of Physics and Astronomy, Cardiff University, Cardiff, UK

1 INTRODUCTION

Much of the research undertaken on classical guitars has been focused on admittance measurements (velocity per unit force) and studies of individual modes of vibration using holographic techniques or modal analysis. Studies have been made on the power input and output from classical guitars but these have been over a low frequency range[1], up to 550 Hz, in front of the instrument or at single frequencies[2]. Sound radiation fields have been investigated to a greater extent but typically only at single frequencies for well separated modes. The sound fields have been studied in terms of their radiativity, which is the sound pressure divided by the applied force. These studies have often been made in combination with holographic interferometery[3] which shows the motion of the instrument from individual modes of vibration. In this paper results are presented showing the radiation efficiency of three guitars and the changing shape of radiativity fields with increasing frequency.

The three guitars are named BR2, BR1 and MAL. BR2 and BR1 are both handmade Torres style classical guitars made by the same luthier. BR2 is described as being a stronger playing instrument than BR1. Both BR1 and BR2 have been used extensively for research in the acoustics group in Cardiff. MAL is a factory made instrument of unknown origin and has a much weaker sound than BR2 and BR1 particularly in the low frequency range.

2 RADIATION EFFICIENCY THEORY

2.1 Radiation Efficiency

Radiation efficiency, η, is a term that has been used by various authors to describe somewhat different variables, but in this paper it is defined as the ratio of mechanical power input to acoustical power output. This is the same definition used by Lai & Burgess[1] for their measurements on guitars and by Suzuki[4] for measurements on a piano soundboard.

2.2 Mechanical Power Input

The power input, at a frequency, ω, is measured by taking the cross power spectrum of the measured force, $F(\omega)$, and velocity, $v(\omega)$, at the same point on the instrument.

$$P(\omega) = Re[F^*(\omega)v(\omega)]$$

$F^*(\omega)$ is the complex conjugate of the measured force. In this work the velocity was measured by integrating the signal from an accelerometer and the force was measured and provided at the same time using an instrumented impact hammer. By using impulse excitation rather than driving individual modes of vibration, a wide range of frequencies are excited in a short amount of time. However it is not possible to drive individual modes of vibration using this method. Using impulse

excitation, any measurements made at a particular frequency will be a combination of several different modes rather than a single isolated mode.

2.3 Acoustical Power Output

Power output is a more complicated measurement than the power input. There are several techniques for calculating the output power generated by an instrument including measuring the sound intensity at varying points around it. Sound intensity using a single microphone can only be measured for plane or spherical waves. As musical instruments typically radiate in non-spherical forms with dipoles, quadrupoles and other higher order components contributing to the radiated sound, this technique is not applicable. At distances much greater than the wavelength of the emitted sound, sound waves may be treated as being planar in nature. However due to restrictions imposed by the wavelengths of sound at low frequencies and also by the size of anechoic rooms, it is not often possible to make use of this simplification.

The method used to calculate the power output in this paper utilised spherical-harmonic decomposition. This requires the measurement of sound pressure using two microphones at a constant separation. The measurements are made on two concentric measurement spheres around the instrument. By measuring the sound pressure with two microphones it is possible to distinguish between the outgoing sound waves from the instrument and any incoming waves. As it is only the outgoing waves that are of interest and importance for analysing the output power of the instrument, measurements were made in an anechoic chamber. This reduces the effect of reflections from the walls of the room or noise from extraneous noise sources and therefore reduces the magnitude of incoming sound waves. Incoming sound waves will still be present due to reflections from support structures, for the guitar and microphones, in the anechoic chamber but by keeping these supports thin and as small as possible the reflections will be minimised.

The sound pressure must be measured at a suitable number of points to describe and analyse the radiated sound field from the instrument. If it is assumed that only monopole (ℓ = 0 in spherical harmonic terms) radiation is generated then a single microphone location will suffice. For this work the system was deliberately over-designed to allow measurements up to ℓ = 9, with sound pressure measurements at 36 azimuth angles and 9 elevation angles. Even though only spherical contributions with $\ell \leq 2$ were investigated, by measuring at more locations the measured and reconstructed fields have a higher resolution and give a clearer visualisation of the sound radiation fields.

The full method for spherical-harmonic decomposition is covered elsewhere in the literature[3, 5] but a brief summary is provided here. The pressure, $p(r,\theta,\varphi)$ at a point on a measurement sphere at a radius, r, from a vibrating object can be described as a combination of incoming and outgoing waves[6].

$$p(r,\theta,\varphi) = \sum_{lm} [a_{lm} h_l(kr) + b_{lm} h_l^*(kr)] Y_{lm}(\theta,\varphi)$$

Here a_{lm} is the outgoing wave coefficient, b_{lm} is the incoming wave coefficient, $h_l(kr)$ is the spherical Hankel function of the first kind, k is the wave number and $Y_{lm}(\theta,\varphi)$ is a spherical harmonic. This equation shows that the incoming and outgoing coefficients have no directional dependence. By measuring sound pressure with two microphones at two different radii, r_1 and r_2, it is possible to solve the two equations simultaneously to calculate a_{lm} and b_{lm}.

$$\begin{bmatrix} a_{lm} \\ b_{lm} \end{bmatrix} = \begin{bmatrix} h_l(kr_1) & h_l{}^*(kr_1) \\ h_l(kr_2) & h_l{}^*(kr_2) \end{bmatrix}^{-1} \begin{bmatrix} C_{lm}(r_1) \\ C_{lm}(r_2 \end{bmatrix}$$

The C_{lm} factors are calculated using a spherical-harmonic decomposition algorithm from the measured pressure data. By increasing the number of values of l and m used in this equation, the reconstructed pressure will become increasingly similar to the measured value. Using this equation

to describe the pressure leads to inaccuracies when the separation of the microphones is equal to half of the wavelength of the radiated sound. The determinant of the matrix containing the spherical Hankel functions approaches infinity as the microphone separation approaches an integer multiple of the half wavelength. This leads to un-physically large values for the reconstructed sound pressure and the incoming and outgoing coefficients. This only has an effect near to integer multiples of the half wavelength and at other frequencies it does not affect the calculated pressure response or output power.

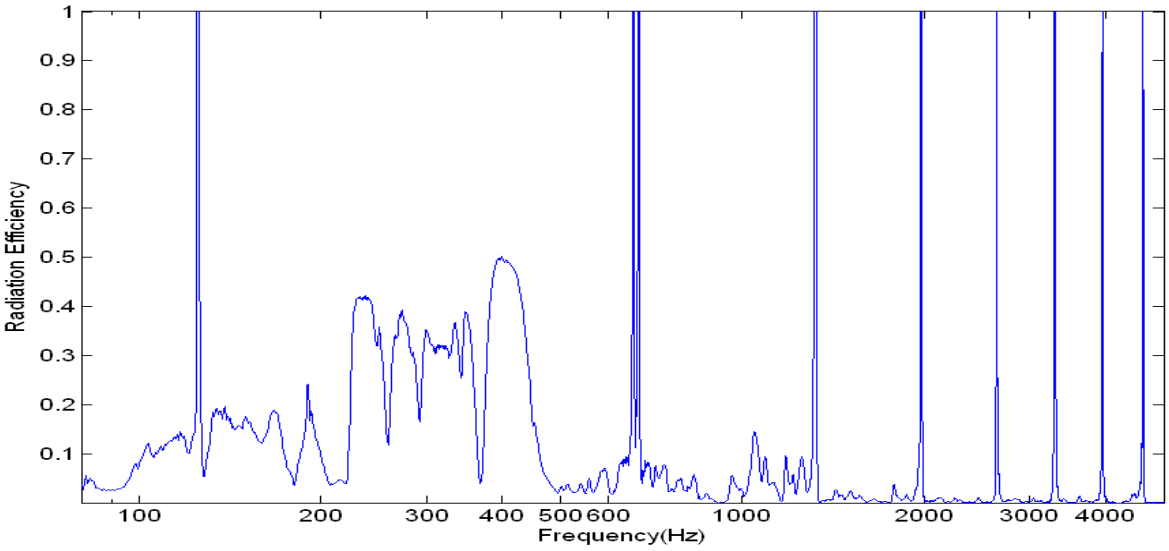

Figure 1. Radiation Efficiency graph for guitar BR2. The spikes are caused by divisions by zero in the inverse spherical Hankel function matrix.

The spikes at multiples of 660Hz in Figure 1 are due to the spherical Hankel functions when integer multiples of half the wavelength is equal or very close in size to the microphone spacing. The spikes are omitted in later graphs. The spike at 120Hz is a result of a low input power measurement leading to an incorrect radiation efficiency value.

The outgoing coefficient, a_{lm} can be used to calculate the source strength, S_ω, of the polar component, from which the total power output, Π, can be calculated[7].

$$\Pi_s = \frac{\rho\omega^2}{4\pi c}|S_\omega|^2$$

In this case, Π_s is the power output from a monopole, ρ is the air density, ω is the frequency, c is the speed of sound and S_ω is the monopole source strength. Other equations for the higher order polar components are found in reference[7]. These output powers are then either summed together and divided by the input power to give the total radiation efficiency or they can be analysed separately to study the influence of individual polar contributions on radiation efficiency. By using a spherical harmonic approach the output power is calculated for all directions from the instrument. This gives a clearer measurement of the overall radiation efficiency of the instrument. However, beyond monopole radiation it is not possible to separate the output power into single directions.

3 EXPERIMENTAL METHOD

An instrumented, automated impact hammer (PCB model 086E80) was used to excite the instrument on its bridge at the right hand side of the top E string. The response was measured using an accelerometer (PCB model 352B10), located between the top B and E strings, and with two ½" microphones (both B&K type 4165/2619) located on two separate measurement spheres

around the instrument. By placing the hammer and accelerometer close to one another a good approximation to the input admittance can be measured. This measurement is made by first taking a FFT of the integrated accelerometer signal (velocity signal) and force signal, then dividing the velocity by force in the frequency domain. The sound pressure generated from each hammer excitation was measured at 324 points on the surface of the measurement spheres and the corresponding force and acceleration measurements were saved as well. These measurements were all undertaken in an anechoic chamber (dimensions 2m x 2m x 1.5m) which limited the radii of the measurement spheres to 0.45m and 0.71m, with the guitar in the centre of the room. The microphones were moved through the nine elevation angles, which were calculated using Gaussian quadrature, and the guitar was rotated through the 36 points 10° at a time. The recordings from each strike were made for two seconds at a sampling rate of 44.1 kHz and a fast Fourier transform (FFT) of window size 2^{16} was made of the data. The total time taken for measurement was around 2 hours.

4 RESULTS AND DISCUSSION

4.1 Radiation Efficiency

BR2 has been studied by measuring input and transfer admittances on the bridge. The modal frequencies and shapes below 600Hz have also been measured. It has not however been analysed in terms of its power output or sound radiation fields at frequencies away from the well defined modes. The input admittance, also known as the mobility, is frequently studied as it provides a measurement of how the body of a stringed instrument reacts to an excitation force. While it is not explicitly being investigated in this paper it is a powerful measurement and will be used in comparison with measurements of radiation efficiency.

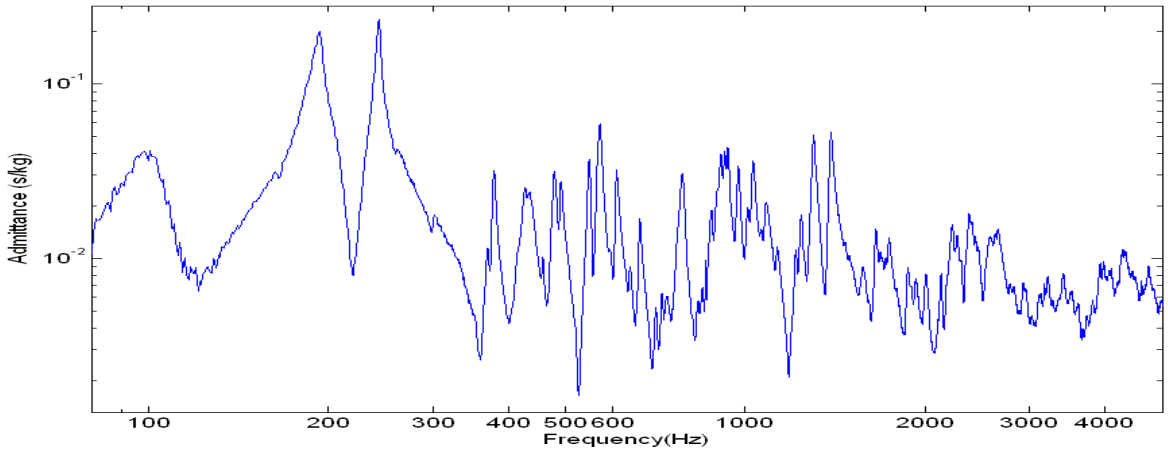

Figure 2. Input admittance graph for guitar BR2 with force excitation and velocity measured at the top E string.

The admittance shown in Figure 2 displays the typical large peaks between 100 Hz and 250 Hz which correspond to the $T(1,1)_1$, $T(1,1)_2$ and T(2,1) modes of vibration. The letter T indicates that the instrument was excited on the top plate. The two numbers indicate the number of anti-nodal regions horizontally (in line with the bridge) and vertically (in line with the strings)[3]. Subscripts are used to denote modes with similar vibration patterns but different phase relationships.

As with most instruments, the admittance has its highest values in the lower frequency range with clearly defined peaks. In the higher frequency region the peaks are far closer to one another. At higher frequencies it is no longer possible to isolate individual modes of vibration as they get nearer one another in frequency.

The data for both graphs in Figure 3 was collected consecutively on the same day to reduce the effect of changes in atmospheric conditions. Figure 3 shows the importance of the sound hole in the generation of sound power with the radiation efficiency between 80 Hz and 200 Hz being considerably reduced when the sound hole is blocked. In both sets of data the regions of increased efficiency between 200 Hz and 500 Hz and between 1 kHz and 1.3 kHz are present. In the input admittance for a guitar with its sound hole blocked, the lowest T(1,1) mode (a Helmholtz resonator type motion) near 100 Hz is missing. The removal of the lowest mode reduces the radiation efficiency. This is to be expected as there are no other modes of similar frequency and higher frequency modes do not contribute much to sound radiation below the resonance frequency.

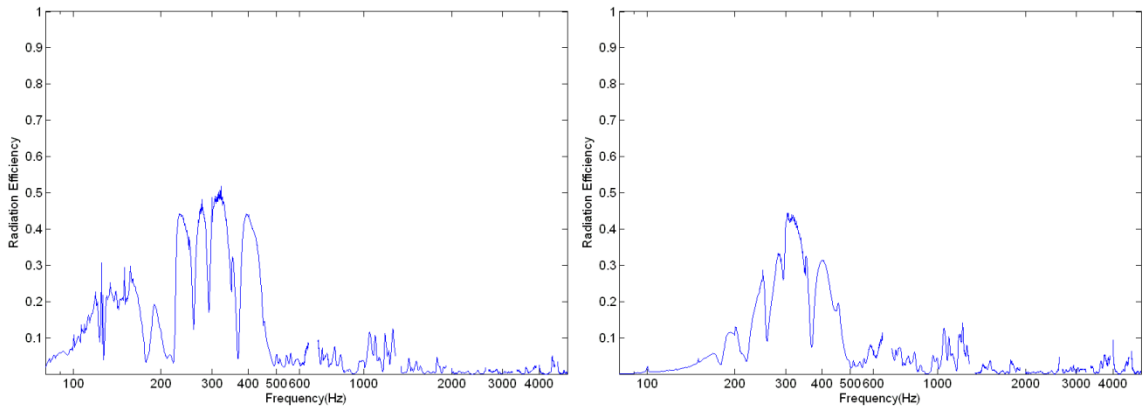

Figure 3. The left hand graph shows the measured radiation efficiency, from all polar contributions, of guitar BR2 with the sound hole open. The right hand graph shows the measured radiation efficiency of guitar BR2 with the sound hole plugged with closed-cell, non-porous foam. The noise at 120Hz for the open sound hole is due to a lower level of input power and output power.

The peaks in the first region of increased efficiency (between 200 Hz and 550 Hz) are slightly lower when the sound hole is blocked compared with when it is open. One possible cause of this effect is that there is an increased resistance provided by the mass of air within the guitar's body acting against the top plate. A further possible cause is that for some higher frequency modes there is a volume change generated within the air cavity by the vibrations of the top plate. The volume change will typically lead to motion out of the sound hole, but if the sound hole is blocked then this is not possible. Depending on the phase relationship between the sound hole and plate vibrations, the radiated sound pressure can either be increased or decreased as a result of the motion. As the radiation efficiency is lower when the sound hole is blocked, it is possible that the plate and sound hole would normally vibrate to increase the sound pressure and output power. The similarities of the radiation efficiencies at frequencies above 600 Hz suggest that the lower frequency air modes are not of great importance in the radiation efficiency at higher frequencies.

For both cases there is a peak in the radiation efficiency at 400 Hz which corresponds to an anti-resonance in the admittance data in Figure 2. The resonance at 379 Hz however has a lower value of radiation efficiency despite having a larger admittance value. This shows that the admittance data is not necessarily an indicator for the values of radiation efficiency.

In Figure 4 it can be seen that the total radiation efficiency below 600 Hz is mainly dependent on monopole sound radiation. The reductions in total radiation efficiency between 200 Hz and 550 Hz correspond with both a reduction in monopole radiation and an increase in dipole radiation. The dips in radiation efficiency appear to be a result of the sound field changing from predominantly monopole radiation to dipole radiation. As the monopole changes into a dipole the total power output decreases due to the dipole being a less efficient radiator than the monopole. The reverse is true for the change from a dipole back to a monopole. These changes are clearly visible in the radiativity sound fields which will be shown in section 4.2.

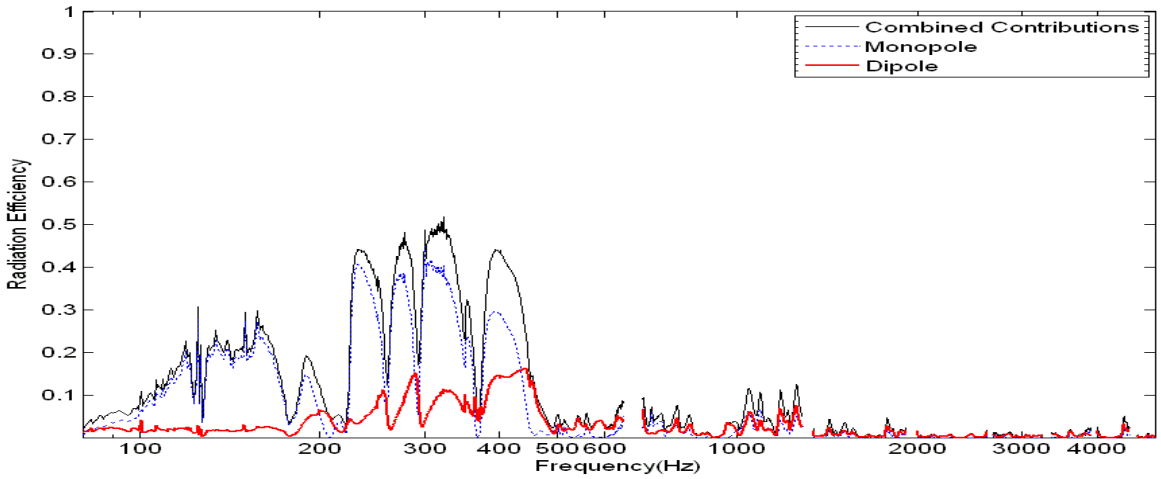

Figure 4. Radiation efficiencies for monopole and dipole components in comparison with the total combined power.

The lowest values of radiation efficiency between 220 Hz and 550 Hz are within a few Hz of the peak values in the admittance. The peaks in admittance correspond to known modes of vibration and above 180 Hz (the $T(1,1)_1$ mode) the patterns of vibration grow increasingly complex. While the two lowest frequency modes are predominantly monopole in nature, from 220 Hz (the T(2,1) mode) there is increasing complexity in the vibrations of the guitar. At higher frequencies the top and back plates of the guitar divide into an increasing number of vibrating regions of alternate phase. This leads to the peaks in the admittance data between 200 Hz and 550 Hz corresponding to modes which behave more like dipoles than monopoles. So while the admittance data shows frequencies where there is a greater level of velocity from the force input, if the vibration drives dipole radiation it will give a lower total output power level.

Quadrupole components and other higher-order modes of vibration have been omitted as they have a considerably lower efficiency and power output than dipoles. The total power radiation efficiency is not noticeably increased by including quadrupole components in the summation and so they have not been included in the figures shown.

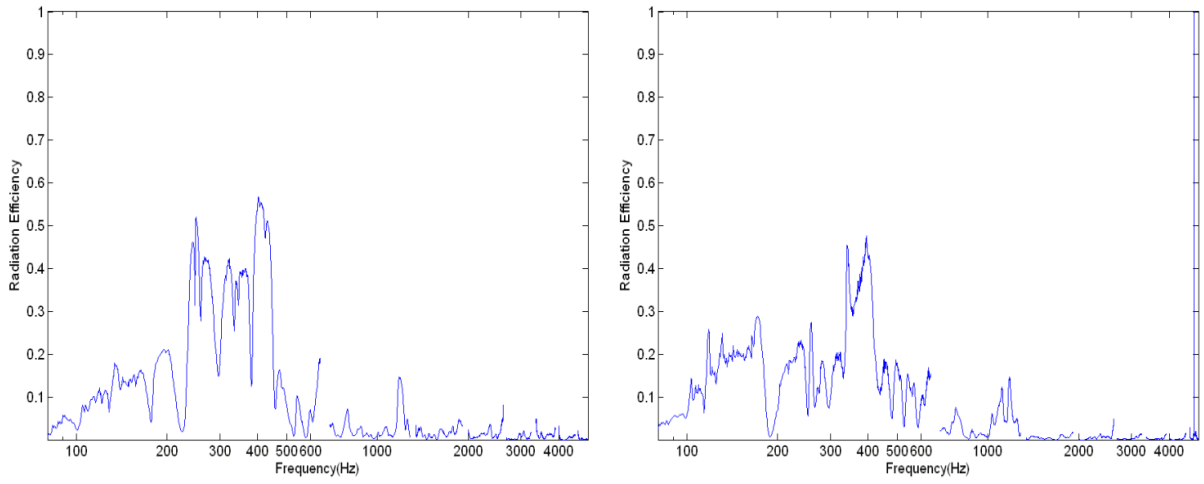

Figure 5. The left hand graph shows the radiation efficiency for guitar BR1. The right hand graph show the radiation efficiency for guitar MAL.

The same patterns in the radiation efficiency between 220 Hz and 500 Hz can be seen both for BR1 and BR2. However below this range BR1 does not radiate quite as efficiently. Guitar MAL is a cheaply made and lower quality instrument and as such it is somewhat "over-constructed" with a thicker top plate in comparison with the other two instruments. While it is less efficient in the region between 200 Hz and 500 Hz it shares some similar characteristics with BR1 and BR2. All three instruments have an increase in radiation efficiency between 300 Hz and 400 Hz and an increase between 1 kHz and 1.3 kHz. A further trend across all three instruments is that at frequencies above 1.3 kHz the radiation efficiency is below 0.05, ignoring noisy data.

MAL has a lower radiation efficiency between 200 Hz and 500 Hz and also above 1.3 kHz. The thicker and stiffer laminated wood used for the top plate of MAL will lead to a smaller value of A/m. A is the effective area of an oscillator and m is the effective mass of the same oscillator[8]. A lower value of A/m leads to a lower level of sound pressure output and therefore a lower acoustic power output. As a result a greater proportion of the power supplied to the instrument at the bridge is lost as heat rather than converted into sound radiation. MAL has a higher radiation efficiency below 200 Hz than either of the other instruments but it is generally agreed to be an instrument of much lower quality. An area for further study, using more instruments, will be whether the region between 200 Hz and 500 Hz may be used as indication of instrument quality as from this small data set it appears to be an indicator.

4.2 Sound Radiation Fields

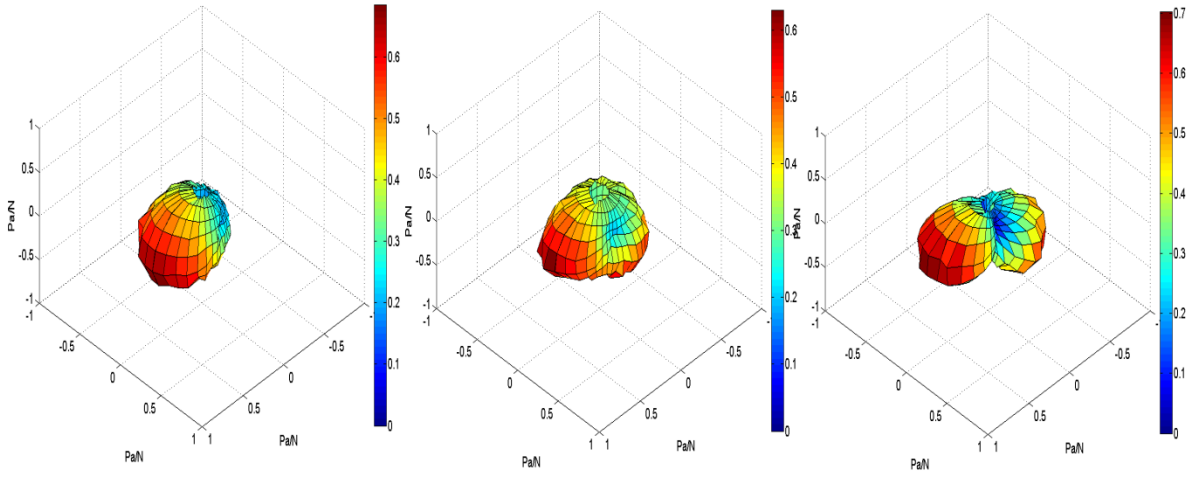

Figure 6. Sound Radiation fields for BR2. From L-R the frequencies are 350Hz, 360Hz and 363Hz. The front of the instrument corresponds to the SW direction, the left to the NW, the right to the SE and the back to the NE.

In Figure 6 the sound radiation field on the left is shown as a strong monopole component with a very small amount of dipole contribution. At 360Hz the dipole begins to develop and contribute a greater amount to the radativity and finally at 363Hz the radiativity is shown as being a strong dipole. The peak values of radiativity are fairly consistent as the frequency changes with a value of around 0.7 Pa/N to the front of the instrument. However the change from a monopole to a dipole, as described above, gives rise to a considerable decrease in the radiation efficiency. The decrease in efficiency is due to the two poles of the dipole working in opposition to one another, so while the peak pressure values do not change the total power output will be much smaller. At 350Hz radiation efficiency is 0.37, at 360Hz it is 0.20 and at 363Hz it is 0.11. The lowest value of radiation efficiency in this region is at 368Hz and has a value of 0.04.

5 CONCLUSIONS

The results show that while an admittance curve will provide data on the frequencies of modes of vibration, higher values in the admittance data are not necessarily an indicator of efficient sound radiation. The main factor which alters the radiation efficiency is whether the radiativity field corresponds to monopole or dipole radiation. As the sound field changes from a monopole to a dipole the total radiation efficiency decreases. All three studied instruments had a higher radiation efficiency between 200Hz and 500Hz and between 1kHz and 1.3kHz. Above this upper frequency the radiation efficiency is always below 5%. The two higher quality instruments, BR1 and BR2, had higher radiation efficiencies between 200Hz and 500Hz than the low quality instrument MAL. This frequency region may be an indicator of quality in an instrument but further measurements on a wider range of guitars is required to confirm this hypothesis.

6 ACKNOWLEDGMENT

We acknowledge financial support from the EPSRC for Ian Perry.

7 REFERENCES

1. J.C.S. Lai and M.A. Burgess, 'Radiation efficiency of acoustic guitars'. Journal of the Acoustical Society of America. 88(3) 1222-1227. (1990)
2. J.A. Torres and R.R. Boullosa, 'Radiation efficiency of a guitar top plate linked with edge or corner modes and intercell cancellation'. Journal of the Acoustical Society of America. 130(1) 546 - 556. (2011)
3. T.J.W. Hill, B.E. Richardson, and S.J. Richardson, 'Acoustical Parameters for the Characterisation of the Classical Guitar'. Acta Acustica United with Acustica. 90 335 - 348. (2004)
4. H. Suzuki, 'Vibration and sound radiation of a piano soundboard'. Journal of the Acoustical Society of America. 80(6) 1573 - 1582. (1986)
5. S.J. Richardson, Acoustical Parameters for the Classical Guitar. PhD thesis, Cardiff University. (2001).
6. G. Weinreich and E.B. Arnold, 'Method for measuring acoustic radiation fields'. Journal of the Acoustical Society of America. 68(2) 404 - 411. (1980)
7. P.M. Morse and K.U. Ingard. Theoretical Acoustics, 1st ed McGraw-Hill. (1968).
8. O. Christensen, 'An Oscillator Model for Analysis of Guitar Sound Pressure Response'. Acustica. 54 289-295. (1984)